

RESEARCH ARTICLE | MARCH 26 2025

Ultra-long-range Bessel beams via leaky waves with mitigated open stopband

E. Negri ; F. Giusti ; W. Fuscaldo ; P. Burghignoli ; E. Martini ; A. Galli 



Appl. Phys. Lett. 126, 121703 (2025)
<https://doi.org/10.1063/5.0253371>



Articles You May Be Interested In

TE-polarized leaky-wave beam launchers: Generation of Bessel and Bessel–Gauss beams

Appl. Phys. Lett. (October 2024)

Microwave generation of X-waves by means of a planar leaky-wave antenna

Appl. Phys. Lett. (October 2018)

Topological wireless communication in the stopband of magnetoinductive lines

J. Appl. Phys. (June 2023)

AIP Advances

Why Publish With Us?



21DAYS
average time
to 1st decision



OVER 4 MILLION
views in the last year



INCLUSIVE
scope

[Learn More](#)



Ultra-long-range Bessel beams via leaky waves with mitigated open stopband

Cite as: Appl. Phys. Lett. **126**, 121703 (2025); doi: [10.1063/5.0253371](https://doi.org/10.1063/5.0253371)

Submitted: 16 December 2024 · Accepted: 13 March 2025 ·

Published Online: 26 March 2025



View Online



Export Citation



CrossMark

E. Negri,^{1,2,a)} F. Giusti,³ W. Fuscaldo,² P. Burghignoli,¹ E. Martini,³ and A. Galli¹

AFFILIATIONS

¹Department of Information Engineering, Electronics and Telecommunications, Sapienza University of Rome, 00184 Rome, Italy

²Istituto per la Microelettronica e Microsistemi, Consiglio Nazionale delle Ricerche, 00133 Rome, Italy

³Department of Information Engineering and Mathematics, University of Siena, 53100 Siena, Italy

^{a)} Author to whom correspondence should be addressed: edoardonegri@cnr.it

ABSTRACT

Open stopband (OSB) mitigation techniques are commonly used to improve the far-field radiating properties of leaky-wave antennas based on periodic structures. Recently, leaky waves have been proposed to focus energy in the near field through Bessel beams. However, the focusing character of Bessel beams is notably limited to a maximum distance known as the *nondiffractive range*. In this work, an OSB mitigation technique is originally exploited to significantly extend the nondiffractive range of a Bessel beam generated by a leaky-wave launcher in the microwave/millimeter-wave range. A comprehensive analysis of this device is presented, comparing the performance of the proposed launcher with the typical structure of a leaky-wave Bessel-beam launcher where the OSB is not suppressed. Theoretical results, corroborated by full-wave simulations, demonstrate that the proposed device achieves an impressive nondiffractive range of about 25 m. The latter, at 30 GHz, approximately corresponds to 2500 wavelengths (in vacuum) and to 50 times the aperture diameter which is about 50 cm. These results look particularly attractive for, e.g., near-field communications and wireless power transfer applications, where focusing energy in narrow regions and over large distances is a key factor.

© 2025 Author(s). All article content, except where otherwise noted, is licensed under a Creative Commons Attribution-NonCommercial-NoDerivs 4.0 International (CC BY-NC-ND) license (<https://creativecommons.org/licenses/by-nc-nd/4.0/>). <https://doi.org/10.1063/5.0253371>

Any kind of wave naturally spreads its energy progressively in all directions during propagation due to diffraction.¹ For this reason, efforts have been made to focus the transmitted power of the wave in specific directions both in the acoustic^{2–4} and electromagnetic^{5–9} regime. In particular, a focused electromagnetic beam is crucial to avoid transmitting power in undesired areas in many practical scenarios, such as secure communications,^{10,11} radiative near-field wireless power transmission,^{12,13} and imaging.¹⁴

In this context, Bessel beams (BBs)—propagation-invariant cylindrical-wave solutions of the Helmholtz equation with focusing and self-healing features^{15,16}—have gained significance. However, in practice, the intriguing BB properties are theoretically maintained only up to a finite distance, commonly known as the *nondiffractive range*.¹⁵ It is thus essential to maximize the covered distance across all frequency bands to fully harness the potential of BBs in real-world applications.

Although BBs have been preliminarily studied in optics in the 1980s,¹⁵ the growing need in focusing EM energy at lower frequencies has renewed research in this area. As a result, the last decade has

seen an exponential growth of works exploring both theoretical and experimental aspects of BBs in the microwave/millimeter-wave domain.¹⁷ In these frequency ranges, a planar, cost-effective, single-feeder, and easy-to-fabricate solution is given by *leaky-wave* BB launchers. In particular, *wideband* BB launchers¹⁸ are preferable with respect to their *resonant* counterparts⁸ for achieving a higher nondiffractive range z_{ndr} , due to their inherently larger radiating apertures. In fact, the value of z_{ndr} scales linearly with the aperture radius ρ_{ap} . By exploiting a ray-optics approximation,¹⁵ these two quantities are more precisely connected, through the so-called *axicon angle* θ_0 , by the equation $z_{\text{ndr}} = \rho_{\text{ap}} \cot \theta_0$.

The axicon angle represents the pointing direction of the rays emerging from the BB aperture with respect to the vertical z axis (see Fig. 1). The closer the rays align with the broadside direction, implying that the axicon angle approaches zero, the larger the nondiffractive range. As reported in the literature,^{8,18} the θ_0 value in leaky-wave launchers is related to the complex radial wavenumber $k_\rho = \beta - j\alpha$, with β and α being the so-called leaky phase and attenuation constants, respectively. Since one typically has that $\theta_0 = \arcsin(\beta/k_0)$ (with k_0

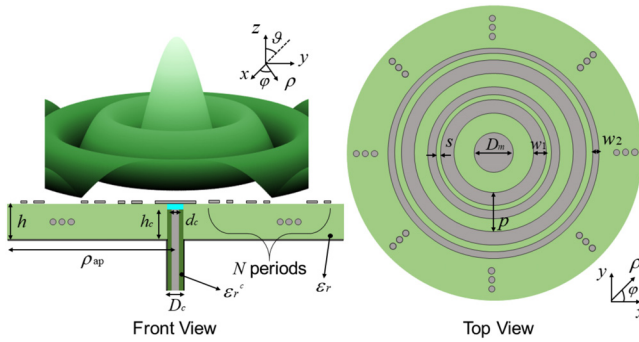


FIG. 1. Front and top view of the proposed wideband BB launcher based on a double asymmetric strip, with a pictorial representation of the excited E_z field distribution. While different green areas represent the different dielectric permittivities of the coaxial cable and of the grounded dielectric slab, light blue and gray colors are associated with vacuum and metal, respectively.

being the vacuum wavenumber), the nondiffractive range can be enhanced by reducing the radial phase constant as much as possible, while keeping the α value sufficiently small, but not vanishing.^{19–21}

However, in conventional wideband BB launchers, when β tends to zero, the value of α changes rapidly: first, it exhibits a highly peaked behavior due to an accumulation of reactive energy, and then drops to zero at the broadside frequency.²² This behavior is attributed to the open stopband (OSB) phenomenon, which arises from the coupling between a pair of oppositely directed spatial harmonics. Different techniques were investigated to mitigate or suppress the OSB, thereby improving the *far-field* radiating properties of 1D leaky-wave antennas.^{23–26} In particular, a longitudinal asymmetry design principle was applied²⁵ using two similar but *unequal* discontinuities inside the unit cell.²⁷

In this work, an OSB mitigation technique has been originally exploited in a 2D, radially periodic, leaky-wave radiating device to improve the *near-field* properties of the generated beam. In particular, a radial unit cell with a *double asymmetric discontinuity* has been considered to extend as much as possible the nondiffractive range of a BB. In order to prove the effectiveness of the proposed design, we compare this structure with a typical wideband BB launcher¹⁸ based on a *single discontinuity* where the OSB is present. A comprehensive Bloch analysis of the two unit cells is performed using the transfer-matrix method to compute the real and imaginary parts of the relevant leaky wavenumber.^{28–30} It is shown that the BB launcher based on the double-discontinuity configuration is able to generate a BB distribution over an impressively long range. With an aperture radius of 24.18 cm, the maximum nondiffractive distance around 30 GHz reaches nearly 25 m, namely, 50 times the aperture diameter and $2500\lambda_0$, with $\lambda_0 = 1$ cm being the vacuum wavelength at the central frequency $f_0 = 30$ GHz. The leaky-wave theoretical results are compared with full-wave simulations, showing a remarkable agreement between the two approaches.

The analysis starts with the design of the wideband BB launchers and the evaluation of their performance through the leaky-wave theory.²⁰ The structures considered in this work are radially periodic leaky-wave radiators constituted by a grounded dielectric slab (with relative permittivity $\epsilon_r = 3.02$, negligible losses, and thickness $h = 1.4$ mm) with an annular metal strip grating on top realized

through standard photolithography⁷ or printed-circuit-board¹⁸ processes. As a consequence, the device performance is strictly related to the leaky phase and attenuation constants.²⁰ The main innovative contribution of this work is the use of an asymmetric double-strip unit cell able to mitigate the OSB²⁷ to enhance the z_{ndr} value: the OSB mitigation is indeed a crucial feature for the generation of long-nondiffractive-range BB since it allows to achieve a non vanishing, sufficiently small, leakage constant α as the leaky phase constant $\beta \rightarrow 0$.

In order to assess the effectiveness of the OSB mitigation in terms of nondiffractive-range enhancement, the Bloch analysis of the constituent unit cell is performed using the transfer-matrix method.^{28–30} To this end, the linearized 1D counterpart of the structure has been considered.^{18,31} Two different case studies are analyzed: the first unit cell has two asymmetric strips of width $w_1 = 1.07$ mm and $w_2 = 0.86$ mm separated by a distance $s = 2$ mm (see Fig. 1), whereas the second unit cell has a single strip of width $w_s = w_1 + w_2$ (see Fig. 2). In both cases, the period is equal to $p = 7.8$ mm.

For this analysis, two waveguide ports with a height of $5.6\lambda_0$ are defined along the periodicity direction. Perfect magnetic boundaries are assigned along y (see insets in Fig. 2) so that a TM mode propagates along the structure. For both cases, transfer matrix of the single unit cell is extracted with CST full-wave simulations by multiplying the transfer matrix obtained simulating $N = 8$ unit cells with the inverse of the one of $N = 7$ unit cells.²⁸ Additional unit cells in the CST simulation may introduce numerical noise with a possible negative impact on the accuracy of the results.³²

The results of the Bloch analysis of the single-strip symmetric unit cell are reported with green curves in Fig. 2. For convenience, both phase and attenuation constants are normalized with respect to the vacuum wavenumber k_0 and indicated as $\hat{\beta} = \beta/k_0$ and $\hat{\alpha} = \alpha/k_0$, respectively. The previously described OSB effect can be clearly seen both in the perturbation of $\hat{\beta}$ and in the null of $\hat{\alpha}$ at the broadside frequency of 30.4 GHz. In contrast, the dispersion curves for the proposed double-strip asymmetric unit cell, shown as black curves in the same figure for comparison, exhibit a mitigated OSB effect, evident as a minor perturbation in both $\hat{\beta}$ and $\hat{\alpha}$ near the broadside frequency.

Once the dispersion curves of the leaky phase and attenuation constants are retrieved, it is possible to theoretically evaluate the performance of the proposed BB launcher. In uniform radiating apertures, the BB nondiffractive range is given by the well-known ray-optics approximation $z_{\text{ndr}} = \rho_{\text{ap}} \cot\theta_0$.⁵ However, the actual nondiffractive range of a leaky-wave BB slightly differs from the ideal one since it is affected by the exponentially damped aperture-field profile. In particular, by indicating the normalized aperture radius as $\bar{\rho}_{\text{ap}} = \rho_{\text{ap}}/\lambda_0$, it reads¹⁹

$$z_{\text{ndr}}^{\text{LW}} = \begin{cases} z_{\text{ndr}} \frac{\ln \sqrt{2}}{\pi \hat{\alpha} \bar{\rho}_{\text{ap}}}, & \frac{\ln \sqrt{2}}{\pi \bar{\rho}_{\text{ap}}} < \hat{\alpha} \ll 1, \\ z_{\text{ndr}}, & \hat{\alpha} \leq \frac{\ln \sqrt{2}}{\pi \bar{\rho}_{\text{ap}}} \ll 1. \end{cases} \quad (1)$$

It is worth noting that while the upper limit $\hat{\alpha} \ll 1$ is required for a physically meaningful leaky wave, the switching condition between the two $z_{\text{ndr}}^{\text{LW}}$ definitions, $\hat{\alpha} = \ln \sqrt{2}/(\pi \bar{\rho}_{\text{ap}})$, is imposed to avoid nonphysical cases for which $z_{\text{ndr}}^{\text{LW}} > z_{\text{ndr}}$.¹⁹

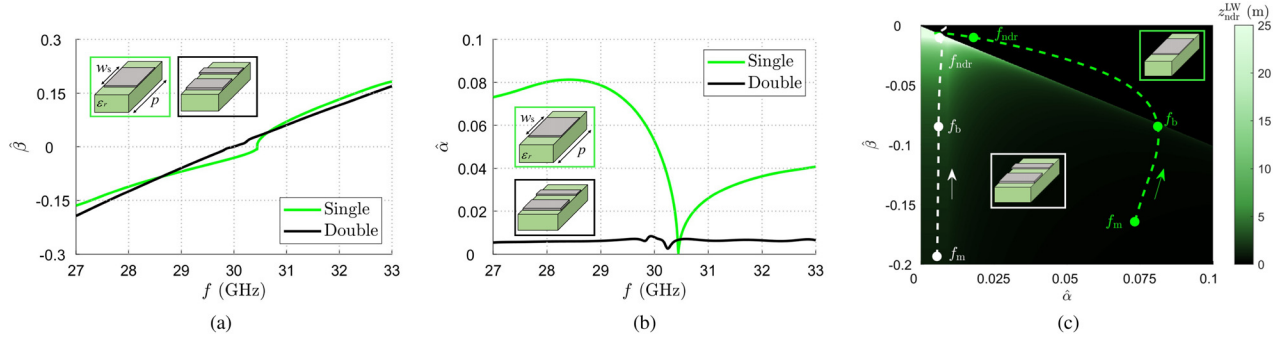


FIG. 2. Bloch analysis of the single-strip symmetric (green curves) and double-strip asymmetric [black curves in (a) and (b)] unit cells. Leaky (a) phase, $\hat{\beta}$, and (b) attenuation, $\hat{\alpha}$, constants normalized with respect to the vacuum wavenumber k_0 are reported vs frequency f . (c) Colormap of the leaky-wave nondiffractive range ($z_{\text{ndr}}^{\text{LW}}$) as a function of the normalized leaky phase, $\hat{\beta}$, and attenuation, $\hat{\alpha}$, constants. The white and green dashed lines represent the synthesized $\hat{\beta}$ and $\hat{\alpha}$ values as the frequency varies (f increases in the arrow direction) for the double- and single-strip unit-cell configurations, respectively. Three interesting frequency points f_m , f_b , and f_{ndr} (see their definitions in the main text) are here marked. As a reference, the unit-cell representation of each considered case is linked to the corresponding curve in a color-code manner.

The axicon angle θ_0 is commonly evaluated in leaky-wave BB launchers through the normalized leaky phase constant by exploiting the simple ray-optics approximation: $\theta_0 = \arcsin \hat{\beta}$.^{18,20} However, in this work, since $\hat{\beta}$ tends to zero for maximizing z_{ndr} , the contribution of the normalized leaky attenuation constant is nonnegligible and it has to be considered for evaluating the leaky-wave pointing angle through³³

$$\theta_0 = \arcsin \sqrt{\hat{\beta}^2 - \hat{\alpha}^2}. \quad (2)$$

At this point, given $\rho_{\text{ap}} = 24.18$ cm, the nondiffractive range $z_{\text{ndr}}^{\text{LW}}$ of a generic leaky-wave BB launcher can be computed through (1) with the z_{ndr} evaluation by means of the definition of the axicon angle in (2). As shown in Fig. 2(c), the nondiffractive range reaches its maximum value of about 25 m (approximately 50 times the aperture diameter and $2500 \lambda_0$) for the considered case study of a double-strip unit cell when both $\hat{\beta}$ and $\hat{\alpha}$ are small and nonvanishing. It is worthwhile to point out that, when $|\hat{\beta}| < \hat{\alpha}$ [see black region in Fig. 2(c)], we are working in the *reactive regime* of the propagating leaky wave (see³⁴ for further details), and thus, we do not consider the possibility to properly generate a BB.

The considered single- and double-strip unit-cell configurations are able to excite a leaky mode whose frequency-dispersive behavior is represented by the green and white curves shown in Fig. 2(c), respectively. These latter are displayed starting from the minimum considered frequency $f_m = 27$ GHz in the region where an backward cylindrical leaky wave is achieved ($\hat{\beta} < 0$ and $\hat{\alpha} > 0$). From a closer inspection of Fig. 2(c), the importance of the OSB suppression is clear: the double-strip unit-cell configuration admits a leaky wavenumber with simultaneously low and flat values for $\hat{\beta}$ and $\hat{\alpha}$ and, in turn, very high nondiffractive-range values. Conversely, the single-strip unit cell, due to the OSB effect, shows large and rapidly changing $\hat{\alpha}$ values when $\hat{\beta} \rightarrow 0$, thus preventing the generation of a BB over a wide spatial region (the green dashed curve mainly falls in the black, reactive region with $|\hat{\beta}| < \hat{\alpha}$). In this case, the best working condition is at the frequency $f_b = 28.6$ GHz, where $|\hat{\beta}| \simeq \hat{\alpha}$, with $\hat{\beta} = -0.084$ and $\hat{\alpha} = 0.081$, corresponding to $z_{\text{ndr}}^{\text{LW}} = 0.34$ m. The same $\hat{\beta}$ is obtained at the same working frequency for the double-strip case with a much

lower attenuation constant ($\hat{\alpha} = 0.006$) thanks to the OSB mitigation; in this manner, a $z_{\text{ndr}}^{\text{LW}} = z_{\text{ndr}} = 2.87$ m is achieved, which clearly shows the detrimental effect of large $\hat{\alpha}$ values in the generation of long nondiffractive ranges. It is, however, important to note that the attenuation constant value also affects the radiation efficiency of the BB launcher through the formula $\eta_r = 1 - e^{-4\pi\hat{\alpha}\rho_{\text{ap}}/\lambda_0}$.²⁰ Therefore, a large aperture radius in terms of wavelengths (here $\rho_{\text{ap}} \simeq 24.18\lambda_0$) is needed as the α value decreases to reach a sufficiently high radiation efficiency (here $\eta_r \simeq 85\%$).

Another interesting working point is the frequency $f_{\text{ndr}} = 29.79$ GHz (where $\hat{\beta} = -0.01$ and $\hat{\alpha} = 0.006$, for the double-strip unit cell), for which the maximum nondiffractive range of $z_{\text{ndr}} \simeq 25$ m is obtained by the proposed wideband BB launcher, a performance that would be unattainable without mitigating the OSB. The condition for which the same $\hat{\beta}$ is synthesized by the single-strip unit cell falls in the reactive region (viz., $|\hat{\beta}| < \hat{\alpha}$) at $f_{\text{ndr}} = 30.39$ GHz with $\hat{\alpha} = 0.018$. It is worthwhile to point out that the proposed double-strip unit cell is only a case study able to show the importance of suppressing the OSB phenomenon for enhancing the z_{ndr} value. Therefore, larger nondiffractive ranges could be obtained with an optimized unit-cell configuration.

In order to corroborate the above-mentioned generation of a BB over a wide nondiffractive region, the near-field evaluation of the device has been addressed and is reported in Fig. 3. The direct derivation of the electromagnetic-field distribution from the full-wave solver would have been computationally expensive due to the very large extension of the spatial domain. For this reason, the simulation of a 3D model of the device has been applied to compute the full-wave *aperture-field distribution*. As is well known, once the tangential aperture-field profile is derived, the equivalence theorem can be applied to find the equivalent electric and magnetic surface currents on the aperture plane.³⁵ At that point, the near-field distribution is computed through the Huygens–Fresnel radiation integral (see, e.g., Ref. 20 for the field-evaluation procedure).

As shown in Fig. 1, a simple coaxial cable penetrating the ground plane of the structure is considered for the proper generation of the BB at microwave/millimeter-wave frequencies (in the terahertz range, one should make use of a mode converter due to the lack of coaxial feeders

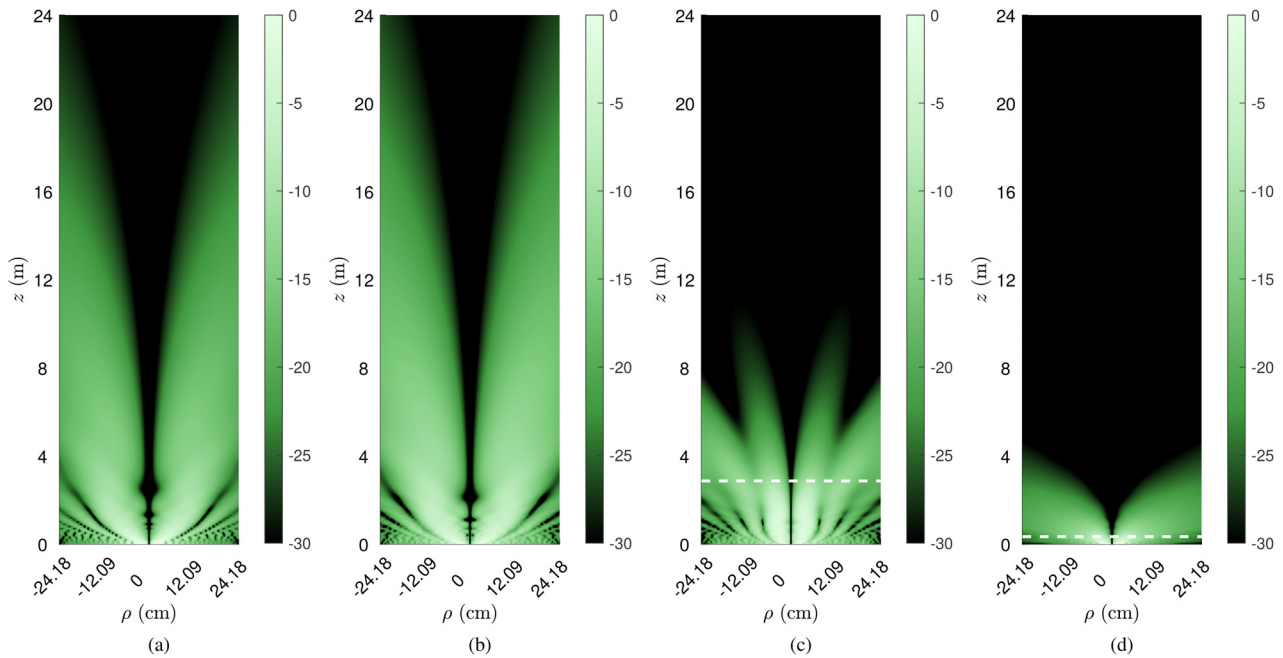


FIG. 3. Colormap in dB of the electric-field radial component—normalized with respect to its maximum—obtained through the radiation integral of the (a) leaky-wave and (b) full-wave aperture-field distributions for the double-strip unit-cell configuration at $f = f_{\text{ndr}}$. The full-wave evaluation of the same field component is shown for the case of a (c) double- and (d) single-strip unit cell at $f = f_b$ (the leaky-wave nondiffractive range is represented through a white dashed line).

at such high frequencies⁷). This source is able to excite a transverse-magnetic (TM) polarized field. While the dielectric permittivity $\epsilon_r^c = 2.1$ and the dimensions of the coaxial cable conductors ($D_c = 0.99$ mm and $d_c = 0.31$ mm—see Fig. 1) are standard, the diameter of a metallic matching disk $D_m = 5.38$ mm and the penetration level of the coaxial cable $h_c = 1.32$ mm in the grounded dielectric slab (drilled at the center with a diameter D_c —see Fig. 1) are tuned for matching purposes. The S_{11} parameter obtained through a full-wave simulation of the double-strip configuration is reported in absolute value (in dB) in Fig. 4, showing a very good impedance matching over the entire frequency band. By using the same feeding scheme for the

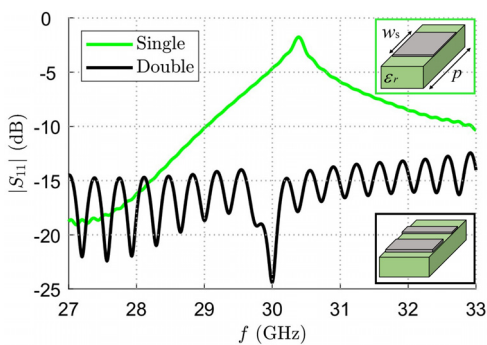


FIG. 4. $|S_{11}|$ (dB) parameter vs frequency f of the proposed long-nondiffractive-range double-strip BB launcher (black solid line—inset on the bottom right corner) and the conventional single-strip BB launcher (green solid line—inset on the top right corner).

single-strip configuration of the wideband BB launcher, a strong mismatch appears around 30.4 GHz. As one can infer from Figs. 2(a) and 2(b), this effect is due to the presence of the OSB because, exactly at this frequency, β and α vanish and, thus, there is an almost total reflection of the propagating wave.^{26,36} Therefore, it is clear that the OSB mitigation is important not only to simultaneously have a small and nonvanishing value of $\hat{\alpha}$ as $\beta \rightarrow 0$, but also to avoid matching issues.

As shown in previous works,^{9,37} a vertical electric dipole (VED) is an accurate model of the above-mentioned coaxial feeders; thus, the total aperture-field distribution is suitably approximated by the azimuthally symmetric, TM-polarized, leaky-wave contribution.³⁸ By considering the leaky-wave aperture field for wideband BB launchers¹⁸ with the leaky phase and attenuation constants in Fig. 2, the theoretical near-field distribution can be computed through the equivalence principle and the Huygens–Fresnel radiation integral.^{19,35}

The results reported in Figs. 3(a) and 3(b) are the near-field distributions of the proposed double-strip wideband BB launcher at $f = f_{\text{ndr}}$, obtained through the radiation integral of the leaky-wave and full-wave aperture-field profiles, respectively. The excellent agreement (with a mean absolute percent error of less than 3%) corroborates both the validity of the leaky-wave analysis through a full-wave simulation and the correct generation of the above-mentioned BB with $z_{\text{ndr}} \simeq 25$ m through an aperture radius $\rho_{\text{ap}} = 24.18$ cm. Figure 3(c) shows the simulated field distribution for the launcher with double-strip unit cells at $f_b = 28.62$ GHz, where $\hat{\beta} = -0.084$ and $\hat{\alpha} = 0.006$. As discussed above, this phase-constant value corresponds to the theoretically “best” working condition for the single-strip unit-cell configuration. Therefore, in Fig. 3(d), the BB generated at $f = f_b$ by the launcher with the typical single-strip unit cell is reported for

comparison. As expected, a leaky-wave nondiffractive range of only 34 cm [white dashed line in Fig. 3(d)] is reached in this case. With the same β , a nondiffractive range $z_{\text{ndr}} = 2.87$ m [see white dashed line in Fig. 3(c)] is achieved thanks to the OSB mitigation provided by the double-strip configuration. Therefore, the importance of the OSB suppression in leaky-wave BB launchers is again clearly visible by a direct comparison of the electric-field distributions in Figs. 3(c) and 3(d).

In conclusion, this work has demonstrated the critical role of open-stopband mitigation in extending the nondiffractive range of leaky-wave wideband Bessel-beam launchers. In particular, this objective has been addressed through the design of an asymmetric double-strip radial unit cell for the annular metal strip grating constituting the radiating aperture of the device, given by a simple grounded dielectric substrate fed by a coaxial probe. The theoretical leaky-wave design remarkably agrees with full-wave simulations, confirming the possibility of generating a Bessel beam over extremely long distances. In particular, with an aperture radius of about 25 cm, a nondiffractive range of approximately 25 m has been achieved—equivalent to 50 times the aperture diameter and 2500 vacuum wavelengths. These findings highlight the potential of Bessel beams for innovative and practical millimeter-wave applications, setting the stage for new advancements in the area of long-distance energy focusing.

E.N. and W.F. acknowledge the project PRIN 2022 “SAFE” (Spiral and Focused Electromagnetic fields) No. 2022ESAC3K, Italian Ministry of University and Research (MUR), financed by the European Union, Next Generation EU. A.G. thanks the support of the European Union under the Italian National Recovery and Resilience Plan (NRRP) of NextGenerationEU, partnership on “Telecommunications of the Future” (No. PE00000001—program “RESTART”).

AUTHOR DECLARATIONS

Conflict of Interest

The authors have no conflicts to disclose.

Author Contributions

E. Negri: Conceptualization (equal); Data curation (equal); Formal analysis (equal); Investigation (equal); Methodology (equal); Resources (equal); Software (equal); Validation (equal); Visualization (equal); Writing – original draft (equal); Writing – review & editing (equal). **F. Giusti:** Conceptualization (equal); Data curation (equal); Investigation (equal); Methodology (equal); Software (equal); Validation (equal); Visualization (equal); Writing – original draft (equal); Writing – review & editing (equal). **W. Fuscaldo:** Formal analysis (equal); Funding acquisition (equal); Investigation (equal); Methodology (equal); Project administration (equal); Resources (equal); Software (equal); Supervision (equal); Validation (equal); Visualization (equal); Writing – review & editing (equal). **P. Burghignoli:** Investigation (equal); Project administration (equal); Resources (equal); Supervision (equal); Writing – review & editing (equal). **E. Martini:** Formal analysis (equal); Project administration (equal); Resources (equal); Supervision (equal); Writing – original draft (equal); Writing – review & editing (equal). **A. Galli:** Formal analysis (equal); Funding acquisition (equal); Project administration (equal); Supervision (equal); Writing – review & editing (equal).

DATA AVAILABILITY

The data that support the findings of this study are available from the corresponding author upon reasonable request.

REFERENCES

- H. E. Hernández-Figueroa, M. Zamboni-Rached, and E. Recami, *Nondiffracting Waves* (John Wiley & Sons, Weinheim, Germany, 2013).
- N. Jiménez, R. Picó, V. Sánchez-Morcillo, V. Romero-García, L. M. García-Raffi, and K. Staliunas, “Formation of high-order acoustic Bessel beams by spiral diffraction gratings,” *Phys. Rev. E* **94**, 053004 (2016).
- M. T. Akram, J.-Y. Jang, and K. Song, “Forward and backward multibeam scanning controlled by a holographic acoustic metasurface,” *Phys. Rev. Appl.* **18**, 024008 (2022).
- K. Song, J. Kim, S. Hur, J.-H. Kwak, S.-H. Lee, and T. Kim, “Directional reflective surface formed via gradient-impeding acoustic meta-surfaces,” *Sci. Rep.* **6**, 32300 (2016).
- J. Durnin, J. J. Miceli, Jr., and J. H. Eberly, “Diffraction-free beams,” *Phys. Rev. Lett.* **58**, 1499 (1987).
- Y. Monnai, D. Jahn, W. Withayachumnankul, M. Koch, and H. Shinoda, “Terahertz plasmonic Bessel beamformer,” *Appl. Phys. Lett.* **106**, 021101 (2015).
- E. Negri, W. Fuscaldo, D. González-Ovejero, P. Burghignoli, and A. Galli, “TE-polarized leaky-wave beam launchers: Generation of Bessel and Bessel-Gauss beams,” *Appl. Phys. Lett.* **125**, 181703 (2024).
- E. Negri, W. Fuscaldo, P. Burghignoli, and A. Galli, “A leaky-wave analysis of resonant Bessel-beam launchers: Design criteria, practical examples, and potential applications at microwave and millimeter-wave frequencies,” *Micromachines* **13**, 2230 (2022).
- M. Ertorre and A. Grbic, “Generation of propagating Bessel beams using leaky-wave modes,” *IEEE Trans. Antennas Propag.* **60**, 3605–3613 (2012).
- D. Bodet, V. Petrov, S. Petrushkevich, and J. M. Jornet, “Sub-terahertz near field channel measurements and analysis with beamforming and Bessel beams,” *Sci. Rep.* **14**, 19675 (2024).
- I. V. Reddy, D. Bodet, A. Singh, V. Petrov, C. Liberale, and J. M. Jornet, “Ultrabroadband terahertz-band communications with self-healing Bessel beams,” *Commun. Eng.* **2**, 70 (2023).
- E. Negri, W. Fuscaldo, P. Burghignoli, and A. Galli, “Leaky-wave analysis of TM-, TE-, and hybrid-polarized aperture-fed Bessel-beam launchers for wireless power transfer links,” *IEEE Trans. Antennas Propag.* **71**, 1424–1436 (2023).
- J. D. Heeb, M. Ertorre, and A. Grbic, “Wireless links in the radiative near field via Bessel beams,” *Phys. Rev. Appl.* **6**, 034018 (2016).
- C. Liu, Z. Zhao, C. Jin, Y. Xiao, G. Gao, H. Xie, Q. Dai, H. Yin, and L. Kong, “High-speed, multi-modal, label-free imaging of pathological slices with a Bessel beam,” *Biomed. Opt. Express* **11**, 2694–2704 (2020).
- J. Durnin, “Exact solutions for nondiffracting beams. I. The scalar theory,” *J. Opt. Soc. Am. A* **4**, 651–654 (1987).
- D. McGloin and K. Dholakia, “Bessel beams: Diffraction in a new light,” *Contemp. Phys.* **46**, 15–28 (2005).
- M. Ertorre, S. C. Pavone, M. Casaletti, M. Albani, A. Mazzinghi, and A. Freni, “Near-field focusing by non-diffracting Bessel beams,” in *Aperture Antennas for Millimeter and Sub-Millimeter Wave Applications* (Springer, Cham, Switzerland, 2018), pp. 243–288.
- D. Comite, W. Fuscaldo, S. K. Podilchak, P. D. Hilarío-Re, V. Gómez-Guillamón Buendía, P. Burghignoli, P. Baccarelli, and A. Galli, “Radially periodic leaky-wave antenna for Bessel beam generation over a wide-frequency range,” *IEEE Trans. Antennas Propag.* **66**, 2828–2843 (2018).
- W. Fuscaldo, A. Benedetti, D. Comite, P. Baccarelli, P. Burghignoli, and A. Galli, “Bessel-Gauss beams through leaky waves: Focusing and diffractive properties,” *Phys. Rev. Appl.* **13**, 064040 (2020).
- W. Fuscaldo, D. Comite, A. Boesso, P. Baccarelli, P. Burghignoli, and A. Galli, “Focusing leaky waves: A class of electromagnetic localized waves with complex spectra,” *Phys. Rev. Appl.* **9**, 054005 (2018).
- E. Negri, F. Giusti, W. Fuscaldo, P. Burghignoli, E. Martini, and A. Galli, “Generation of a long-nondiffractive-range leaky-wave Bessel beam through an open-stopband mitigation technique,” in *International Symposium on Antennas and Propagation (ISAP) 2024* (IEEE, Incheon, Korea, 2024), pp. 1–2.

- ²²A. Hessel, "General characteristics of traveling wave antennas," in *Antenna Theory*, edited by R. E. Collin and F. J. Zucker (Mc-Graw-Hill, New York, 1969), Chap. 19, pp. 151–258.
- ²³P. Burghignoli, G. Lovat, and D. Jackson, "Analysis and optimization of leaky-wave radiation at broadside from a class of 1-D periodic structures," *IEEE Trans. Antennas Propag.* **54**, 2593–2604 (2006).
- ²⁴A. Al-Bassam, S. Otto, D. Heberling, and C. Caloz, "Broadside dual-channel orthogonal-polarization radiation using a double-asymmetric periodic leaky-wave antenna," *IEEE Trans. Antennas Propag.* **65**, 2855–2864 (2017).
- ²⁵J. Liu, W. Zhou, and Y. Long, "A simple technique for open-stopband suppression in periodic leaky-wave antennas using two nonidentical elements per unit cell," *IEEE Trans. Antennas Propag.* **66**, 2741–2751 (2018).
- ²⁶F. Giusti, S. Maci, and E. Martini, "Complete open-stopband suppression using sinusoidally modulated anisotropic metasurfaces," *IEEE Trans. Antennas Propag.* **71**, 8537–8547 (2023).
- ²⁷P. Baccarelli, P. Burghignoli, D. Comite, W. Fuscaldo, and A. Galli, "Open-stopband suppression via double asymmetric discontinuities in 1-D periodic 2-D leaky-wave structures," *IEEE Antennas Wireless Propag. Lett.* **18**, 2066–2070 (2019).
- ²⁸N. Apaydin, L. Zhang, K. Sertel, and J. L. Volakis, "Experimental validation of frozen modes guided on printed coupled transmission lines," *IEEE Trans. Microwave Theory Techn.* **60**, 1513–1519 (2012).
- ²⁹F. Mesa, G. Valerio, R. Rodríguez-Berral, and O. Quevedo-Teruel, "Simulation-assisted efficient computation of the dispersion diagram of periodic structures: A comprehensive overview with applications to filters, leaky-wave antennas and metasurfaces," *IEEE Antennas Propag. Mag.* **63**, 33–45 (2021).
- ³⁰F. Giusti, Q. Chen, F. Mesa, M. Albani, and O. Quevedo-Teruel, "Efficient Bloch analysis of general periodic structures with a linearized multimodal transfer-matrix approach," *IEEE Trans. Antennas Propag.* **70**, 5555–5562 (2022).
- ³¹S. K. Podilchak, P. Baccarelli, P. Burghignoli, A. P. Freundorfer, and Y. M. Antar, "Analysis and design of annular microstrip-based planar periodic leaky-wave antennas," *IEEE Trans. Antennas Propag.* **62**, 2978–2991 (2014).
- ³²E. Negri, W. Fuscaldo, P. Burghignoli, and A. Galli, "An overview of design techniques for two-dimensional leaky-wave antennas," *Appl. Sci.* **15**, 1854 (2025).
- ³³G. Lovat, P. Burghignoli, and D. R. Jackson, "Fundamental properties and optimization of broadside radiation from uniform leaky-wave antennas," *IEEE Trans. Antennas Propag.* **54**, 1442–1452 (2006).
- ³⁴W. Fuscaldo, P. Burghignoli, and A. Galli, "The transition between reactive and radiative regimes for leaky modes in planar waveguides based on homogenized partially reflecting surfaces," *IEEE Trans. Microwave Theory Techn.* **68**, 5259–5269 (2020).
- ³⁵C. A. Balanis, *Advanced Engineering Electromagnetics* (Wiley, 2012).
- ³⁶S. Paulotto, P. Baccarelli, F. Frezza, and D. R. Jackson, "A novel technique for open-stopband suppression in 1-D periodic printed leaky-wave antennas," *IEEE Trans. Antennas Propag.* **57**, 1894–1906 (2009).
- ³⁷M. Ettore, S. M. Rudolph, and A. Grbic, "Generation of propagating Bessel beams using leaky-wave modes: Experimental validation," *IEEE Trans. Antennas Propag.* **60**, 2645–2653 (2012).
- ³⁸A. Ip and D. R. Jackson, "Radiation from cylindrical leaky waves," *IEEE Trans. Antennas Propag.* **38**, 482–488 (1990).